

## Organometallic polymeric carriers for redox triggered release of molecular payloads†

Dominik Jańczewski,<sup>a</sup> Jing Song,<sup>a</sup> Erzsébet Csányi,<sup>b</sup> Lóránd Kiss,<sup>c</sup> Péter Blazsó,<sup>d</sup> Róbert L. Katona,<sup>d</sup> Mária A. Deli,<sup>c</sup> Guillaume Gros,<sup>a</sup> Jianwei Xu<sup>a</sup> and G. Julius Vancso‡\*<sup>a</sup>

Received 9th November 2011, Accepted 12th January 2012

DOI: 10.1039/c2jm15755a

The synthesis and characterization of a novel redox responsive comb-copolymer consisting of a poly(ferrocenylsilane) backbone and *N*-dimethylethyl ammonium and *N*-dimethyldecyl ammonium substituents are reported. Due to the presence of the side groups featuring cationic amine as well as decyl hydrocarbon chains the comb copolymer exhibits amphiphilic behaviour and forms micellar assemblies with typical dimensions of 100 nm. The assemblies display unique, redox induced morphology change in water, investigated by dynamic light scattering and transmission electron microscopy. Paclitaxel and Nile Red were encapsulated in the micelles as model guest molecular payloads. Release of the guests with a high degree of profile control by varying the concentration of redox agents is presented.

## Introduction

Nature provided us with unique, tailored solutions at the nano-scale for molecular delivery and submicrometre compartmentalization. Virus capsids, perfectly crafted for the nucleic acid delivery, or lysosomes, playing a vital role as intracellular reactors, are just some examples of a wide family of naturally occurring vehicles,<sup>1</sup> with sizes of a few dozen nanometres.<sup>2</sup> Drug and biomolecular delivery, which is a traditional field for application of such devices, is looking for nano-containers with the ability to release material upon triggered external stimuli.<sup>3</sup> Improved delivery control could address fundamental issues of contemporary medicine like lowering the effective dose, reducing side effects, as well as providing solutions for an effective way to deliver biomacromolecules. Applications of amphiphilic block-<sup>4</sup> and comb-co-polymers<sup>5</sup> have attracted considerable attention, when molecules for construction of micellar compartments are requested. Their application may become successful for many

types of encapsulation, spanning from inorganic nanoparticles<sup>6</sup> to biologically active organic compounds.<sup>7</sup>

Redox responsive delivery vehicles could provide a suitable solution for the release directly into intracellular compartments with local redox gradient.<sup>8</sup> They may also serve as materials to fabricate devices that respond to variations of the electric potential.<sup>9</sup> There are various ways to incorporate the redox trigger into a molecular delivery vehicle. Obviously, it is necessary for part of the constituting molecules to undergo a reversible or irreversible reduction–oxidation process.<sup>10</sup> Disulfide bridges<sup>11</sup> and ferrocene derivatives,<sup>12</sup> with oxidation potential *versus* standard hydrogen electrode of  $-0.25$  V and  $0.6$  V respectively, are two particularly favourable solutions investigated.

Poly(ferrocenylsilane) (PFS),<sup>13</sup> an interesting class of redox responsive polymers, featuring alternating ferrocene and silicon units within the polymer backbone, was also explored in the context of redox responsive release vehicles.<sup>14</sup> Layer by layer (LbL) structures composed of PFS polyions<sup>15</sup> with alternating charges and block-copolymeric micelles<sup>16</sup> containing the PFS unit were assembled for this purpose.

In this contribution the synthesis and application of novel redox active vehicles, constructed with an amphiphilic PFS comb co-polymer, are reported. The polymer, when suspended in water, forms composite micelles with hydrophobic pockets suitable for molecular delivery purpose. Unlike many redox active systems reported so far, micellar assemblies do not decompose upon redox stimuli but display reversible morphology transformation effectively collapsing and expanding as a molecular sponge. Due to their suitable size, in the 100 nm range, and their positive charge, the properties of the materials are investigated in the context of redox triggered release of drugs and DNA delivery.

<sup>a</sup>Institute of Materials Research and Engineering A\*STAR (Agency for Science, Technology and Research) 3 Research Link, Singapore 117602. E-mail: g.j.vancso@utwente.nl; Fax: +31 53 4893823; Tel: +31 53 489 2974

<sup>b</sup>Department of Pharmaceutical Technology, University of Szeged, Eötvös u. 6, H-6720 Szeged, Hungary

<sup>c</sup>Institute of Biophysics, Biological Research Centre of the Hungarian Academy of Sciences, Temesvári krt. 62, H-6726 Szeged, Hungary

<sup>d</sup>Institute of Genetics, Biological Research Centre of the Hungarian Academy of Sciences, Temesvári krt. 62, H-6726 Szeged, Hungary

† Electronic supplementary information (ESI) available: Cyclic voltammograms and LDH graphs. See DOI: 10.1039/c2jm15755a

‡ Permanent address: Materials Science and Technology of Polymers, Faculty of Science and Technology, University of Twente and MESA+ Institute for Nanotechnology, P. O. Box 217, AE 7500, Enschede, The Netherlands.

## Experimental

### Materials

All reagents were purchased from commercially available sources and were used without further purification.  $^1\text{H}$  NMR and  $^{13}\text{C}$  NMR spectra were obtained with a Bruker spectrometer (DRX 400 MHz). UV-vis absorption and fluorescent spectra were recorded using a Shimadzu spectrophotometer (UV-1601) and a Shimadzu spectrofluorometer (RF-5301PC), respectively. Cyclic voltammetry experiments were obtained using an Autolab setup. Dynamic light scattering (DLS) measurements were performed with a Bruker device equipped with a HeNe 633 nm laser and a scattering angle of  $90^\circ$ . HPLC paclitaxel assay was performed using a Waters setup equipped with a Waters Symmetry Shield RP8 column. GPC analysis was performed using a Waters setup, PLgel 10  $\mu\text{m}$  mixed-B columns and poly (methyl methacrylate) standards as reference. Transmission electron microscopy (TEM) micrographs were recorded with a JEOL 2100 instrument.

### Synthesis of polymer 2

Monomer **1** (10.3 g, 33.7 mmol) was dissolved in dry tetrahydrofuran (THF) (150 mL) and cooled to  $-25^\circ\text{C}$ . Subsequently chloroplatinic acid (0.4 g, 0.78 mmol), dried overnight under vacuum, was added and the reaction mixture was stirred for 24 h in  $-25^\circ\text{C}$ . The polymer solution was precipitated with methanol and centrifuged. After drying 5.1 g of orange polymer flakes were obtained. Chlorine-functionalized PFS was subsequently dissolved in THF and dicyclohexano 18-crown-6 (0.4 g) followed by addition of potassium iodide (4 g). The mixture was vigorously stirred for 7 days and precipitated with methanol. The procedure including dissolution in fresh THF and addition of dicyclohexano 18-crown-6 and potassium iodide was repeated three more times. Intensity changes of  $\text{CH}_2$   $^1\text{H}$  NMR signals, next to  $-\text{Cl}$  and  $-\text{I}$  atoms, were used to follow the progress of the reaction. Final precipitation with methanol and drying resulted in **2** as orange flakes (6.0 g, 46%).  $M_n = 17.5$  kDa,  $M_w = 21.7$ , PDI = 1.2.  $^1\text{H}$  NMR ( $\text{CDCl}_3$ ) integrated for a single repeating unit:  $\delta$ : 4.23 (s, 4H); 4.12–3.95 (m, 4H); 3.28–3.15 (m, 2H); 1.96–1.80 (m, 2H); 1.05–0.96 (m, 2H); 0.48 (s, 3H).

### Synthesis of polymer 3

Polymer **2** (0.42 g, 1.3 mmol r.u.) was dissolved in dry THF (10 mL), and a solution of *N,N*-dimethyldecylamine (0.075 g, 0.4 mmol) was added. The mixture was stirred at RT for 50 h. Subsequently *N,N*-dimethylethylamine (0.6 mL, 12.2 mmol) and 10 mL of dry DMSO were added and stirring was continued for the next 100 h. Volatile solvents were evaporated with a rotary evaporator and the remaining solution in DMSO was dialyzed (DI water,  $3\times$  with a solution of sodium chloride  $0.1\text{ mol L}^{-1}$ ,  $3\times$  with DI water). The concentration and freeze-drying of the solution afforded polymer **3** in the form of dark orange flakes (0.39 g, 76%). Calculated  $M_n = 16.2$  kDa.  $^1\text{H}$  NMR integrated for a single repeating unit: (MeOD)  $\delta$ : 4.45–4.00 (m, 8H); 3.40–3.15 (m, 4H); 3.00 (s, 6H); 1.74 (br, 2H); 1.62 (br, 0.45H); 1.22–1.50 (m, 5.4H); 1.02–0.88 (m, 2.5H); 0.68–0.54 (s, 3H);  $^{13}\text{C}$  NMR (MeOD)  $\delta$ : 74.75, 74.64, 72.98, 72.85, 67.3, 60.9, 51.4, 50.6, 33.1,

30.66, 30.63, 30.47, 30.27, 27.44, 23.79, 23.60, 18.6, 14.6, 13.65, 8.5,  $-3.4$ .

### Redox reversible behaviour of polymeric micelles composed of polymer 3

Reversible oxidation and reduction were carried out using chemical agents. Namely, polymer **3** was oxidized using 2 molar equivalents of iron chloride(III) and reduced back with 1 equivalent of sodium ascorbate. In sequential experiments (multiple reduction/oxidation cycles), the amounts of chemical agents were increased by 5% in every cycle to reassure quantitative transformation. Reversibility of the process was observed with UV-VIS absorbance experiments and DLS.

### Controlled release of Nile Red

Polymer **3** (1.2 mg) and Nile Red ( $3 \times 10^{-4}$  mg) were dissolved in ethanol (3 mL) and stirred for 2 hours. After solvent evaporation at RT in a vacuum oven, and subsequent water addition (3 mL), the mixture was stirred for 2 hours to yield PFS dye loaded micelle suspension. To compare the dye release rates, the micelles were oxidised with iron chloride(III). Three different amounts of  $\text{FeCl}_3$  (1 mg, 2 mg, 3.5 mg) were added into micelle solutions (3 mL) individually. The released dye molecules were monitored by fluorescence.

### Controlled release of paclitaxel

In a typical experiment 12.9 mg of amphiphilic polymer **3** and 4.6 mg of paclitaxel were dissolved in 5 mL of methanol. The solvent was evaporated and the mixture was resuspended in 5 mL water. The solution was transferred into dialysis tubes ( $M_w$  cut-off 3500 Da) and dialysed against 50 mL water, or 50 mL of  $\text{FeCl}_3$  solution (0.14 mM or 0.68 mM). The dialyzing solution was replaced at predetermined time intervals. 5 mL of dichloromethane (DCM) was used to extract the released paclitaxel from water layers. After evaporation of DCM the remaining solid was dissolved in 1.5 mL of the HPLC mobile phase. The concentration of paclitaxel was measured using high performance liquid chromatography (HPLC). HPLC was performed in the isocratic system water/acetonitrile 50 : 50, v/v.

### Cell toxicity study

Toxicity tests were performed as described earlier.<sup>17</sup> Human intestinal epithelial Caco-2 cells (ATCC, USA) were cultured in MEM supplemented with 10% fetal bovine serum, 1% Na pyruvate, and  $50\text{ }\mu\text{g mL}^{-1}$  gentamicin in a humidified incubator with 5%  $\text{CO}_2$  at  $37^\circ\text{C}$ . When cells reached approximately 80–90% confluency in the dish, they were subcultured with a 0.05% trypsin–EDTA solution. For viability and toxicity tests Caco-2 cells were seeded to 96-well plates at a density of  $10^4$  cells per well. During experiments the cells were cultured in Dulbecco's Modified Eagle's Medium (DMEM, Sigma) prepared with or without 5% fetal bovine serum. Polymers **3** and **4** were dissolved in sterile distilled water at a concentration of  $10\text{ mg mL}^{-1}$ . The following dilutions (treating solutions) were prepared in culture medium with or without serum for each PFS: 3, 10, 30, 60, 100, 300 and  $1000\text{ }\mu\text{g mL}^{-1}$ . Untreated cells (control group) received

only the appropriate culture medium. Caco-2 cells grown in 96 well plates for 4 days reached confluence and were used for experiments. For each treatment group 4–8 parallel wells were used. Living cells convert the yellow 3-(4,5-dimethylthiazol-2-yl)-2,5-diphenyltetrazolium bromide (MTT, Sigma) dye to purple formazan crystals. One hour before ending 24 h treatments Caco-2 cells cultured in 96-well plates received  $0.5 \text{ mg mL}^{-1}$  MTT solution and were further incubated in a  $\text{CO}_2$  incubator for three hours. The amount of formazan dye was determined by measuring the absorbance at 595 nm with a microplate reader (Fluostar Optima, BMG Labtechnologies, Germany). The result is shown as the percentage of the control group (100% viability). The release of the cytoplasmic enzyme lactate dehydrogenase (LDH) from cells is a sign of cell membrane damage and can be used as an indicator of cell death. LDH from the culture supernatant was determined by a commercially available cytotoxicity detection kit measuring LDH release (Roche). After treatments for 24 h 50  $\mu\text{L}$  samples from culture supernatants were incubated with equal amounts of reaction mixture for 15 minutes. The enzyme reaction was stopped by 0.1 M HCl. The absorbance was measured at a wavelength of 492 nm with a microplate reader (Fluostar Optima, BMG Labtechnologies, Germany). Cytotoxicity was calculated as the percentage of the total LDH release from cells treated by the 1% Triton X-100 detergent.

### DNA delivery study

Transfection experiments were performed on a CHO-S (Invitrogen) derived, puromycin resistant ChC3 cell line.  $3 \times 10^5$  cells were plated equally in each well of a standard 6-well culturing plate the day before transfection. Cells were maintained in DMEM with high glucose (Gibco 52100) containing 10 v/v% fetal bovine serum (FBS, PAA A15-151), 4 mM stable glutamine (PAA M11-006),  $1 \times$  penicillin/streptomycin (PAA P11-010) and  $5 \mu\text{g mL}^{-1}$  puromycin (Sigma). Cell cultures were kept in a humidified incubator with 5 v/v%  $\text{CO}_2$  at  $37^\circ\text{C}$  during the whole experiment. Red fluorescent protein expressing plasmid DNA (pEF1alpha-tdTomato, Clontech 631975) was used for delivery. Polymers **3** and **4** were previously dissolved in distilled water and sterile filtered using Millex-GP (Millipore) filter units. On the day of DNA delivery 400  $\mu\text{L}$  transfection solutions were prepared the following way: 16  $\mu\text{g}$  polymer or 6  $\mu\text{L}$  Turbofect™ *in vitro* transfection reagent (Fermentas) and 4  $\mu\text{g}$  plasmid DNA were mixed in an appropriate volume of DMEM (Gibco 12491). Control solutions contained only plasmid DNA + DMEM (“no reagent, DNA”) or DMEM alone (“no reagent, no DNA”). After 10 minutes of incubation at room temperature transfection solutions were added to the cells with 3.6 mL of fresh, complete growth medium. Cell cultures were incubated for 24 hours, trypsinized, pelleted and resuspended in phosphate buffered saline (PBS) + 1 v/v% FBS. The red fluorescent signal positivity of 2000 cells in each suspension was measured at  $580 \pm 20 \text{ nm}$  on a Guava PCA (Millipore) flow cytometry system using the Guava Express Assay software module.

## Results and discussion

Synthesis of the amphiphilic PFS polymer was carried out by the ring opening polymerization (ROP)<sup>18</sup> of strained cyclic

ferrocenophane monomer **1**<sup>19</sup> and subsequent exchange of chlorine atom into iodide.<sup>20</sup> Tuning of protocols described previously,<sup>21</sup> mainly by lowering the reaction temperature and drying the catalyst, resulted in oligomeric (average 44 repeating units) PFS product **2** with a low molecular mass  $M_w = 21.7 \text{ kDa}$  and polydispersity index (PDI) = 1.2. Polymer **2** was subsequently functionalized using dimethylethylamine and dodecyldecylamine to form statistical comb-co-polymer **3** bearing hydrophilic and hydrophobic units. The  $^1\text{H}$  NMR spectrum in deuterated methanol shows the structure of polymer **3**, with a percentage of amphiphilic units of 23%, calculated independently using integration of three different proton signals *versus* cyclopentadienyl (Cp) protons. Polymer **4** was synthesized following the same protocol, but using *N,N*-dimethylethylamine only, and was used as a reference for NMR interpretation, the cyto-toxicity study and the DNA delivery (Fig. 1).

Amphiphilic PFS comb-co-polymer **3** is soluble in water and exhibits properties previously reported for the other PFS based materials.<sup>22</sup> It undergoes a reversible reduction–oxidation process when treated with redox agents, which can be carried out for many cycles as demonstrated by UV absorption spectral changes (Fig. 2). The oxidation potential of micellar PFS **3** remains in the region characteristic for other PFS derivatives. In comparison to polymer **4** the typical double oxidation signal is not visible in cyclic voltammetry experiments (see ESI†). Oxidation of polymer **3** leads to the abrupt change of the charge density in the main backbone. Despite the changes of its hydrophobic character (atom number to charge ratio changing from 54 to 27, for reduced and oxidized forms, respectively) polymer **3** remains water suspendable, forming optically transparent solutions in both forms.

Micellar assemblies of polymer **3** do not decompose upon exposure to redox stimuli but display a reversible morphology transformation. To gain further insight into the morphology variation, DLS experiments were performed within several cycles of chemical oxidation and reduction. In both states clear aggregation was visible (Fig. 3). Despite increase in charge density of the main backbone, interactions of decyl chains of hydrophobic subunits were driving aggregation also in the oxidized form. The average diameter of composite micelles remains in the range of 80–120 nm with a small increase upon oxidation of the material.

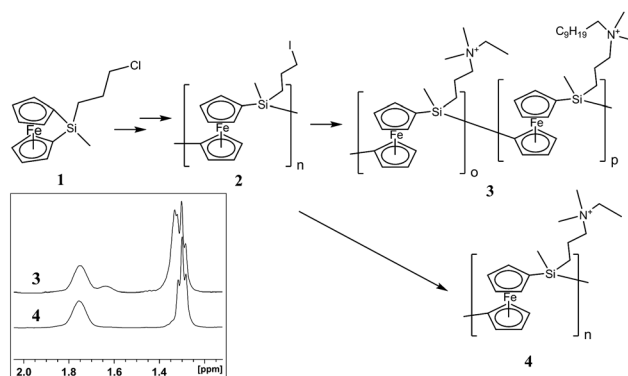


**Fig. 1** Synthesis of polymer **3** and polymer **4**. Indexes based on  $^1\text{H}$  NMR:  $n = 44$ ,  $o = 34$ ,  $p = 10$ . Inset: comparison of NMR signals of polymers **3** and **4** allowing for calculation of the composition of polymer **4**.

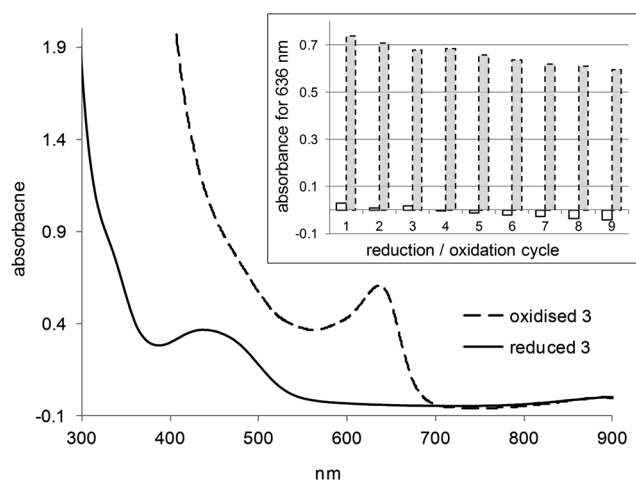


**Fig. 2** Absorption of micellar PFS polymer **3** in oxidized and reduced forms. Inset: variation of the absorbance for reduction–oxidation cycles of the water suspended polymer **3** micelle. Transformations were reversibly induced with iron chloride(III) and sodium ascorbate solutions.

Transmission electron microscopy (TEM) micrographs (Fig. 4) depict small size differences between oxidized and reduced forms of polymer **3**. The overall cluster diameter of 50–80 nm, observable by TEM, is however apparently smaller compared to DLS measurements and could be explained by the dry state of the micelle. Clearly, the morphology is different for the two forms of polymer **3** as visible in TEM, with a less compact structure in the case of the oxidized polymer. Upon five redox cycles a small overall decrease in size was observed by DLS; this could probably be associated with increased ionic strength of the solution upon addition of the redox agents.†

To demonstrate triggered, redox controlled drug release abilities, experiments with two different molecules were carried out. Model fluorescent dye Nile Red and anticancer drug paclitaxel were employed. Nile Red is a molecule known for high environmental sensitivity.<sup>23</sup> It can be applied as a probe to study processes like transition from a hydrophobic to hydrophilic environment accompanied by an abrupt change in fluorescent intensity.

Nile Red was encapsulated into the polymeric PFS micelle of polymer **3** by dissolution in ethanol and evaporation of the solvent. Fig. 5 shows the change of the dye emission intensity of the PFS micelle solution after adding  $\text{FeCl}_3$ . The emission intensity of the dye molecules decreased with time, indicating the release of guest molecules and exposure to a water environment. The higher the concentration of the oxidant, the faster is the drop of fluorescent intensity associated with the release rate. In the control experiment, no  $\text{FeCl}_3$  was added and the intensity remained constant for 9 hours. This result suggests that the micellar solution was stable without releasing the dye during the control experiment.

Paclitaxel is an important chemotherapeutic drug,<sup>24</sup> widely used for treatment of various types of cancer. The low water

† Analyzing the DLS results, it also should be mentioned that DLS measurements of the oxidized form of polymer **3** may be covered with some bias due to the material absorption profile overlapping with the wavelength of the HeNe laser used in the DLS setup.

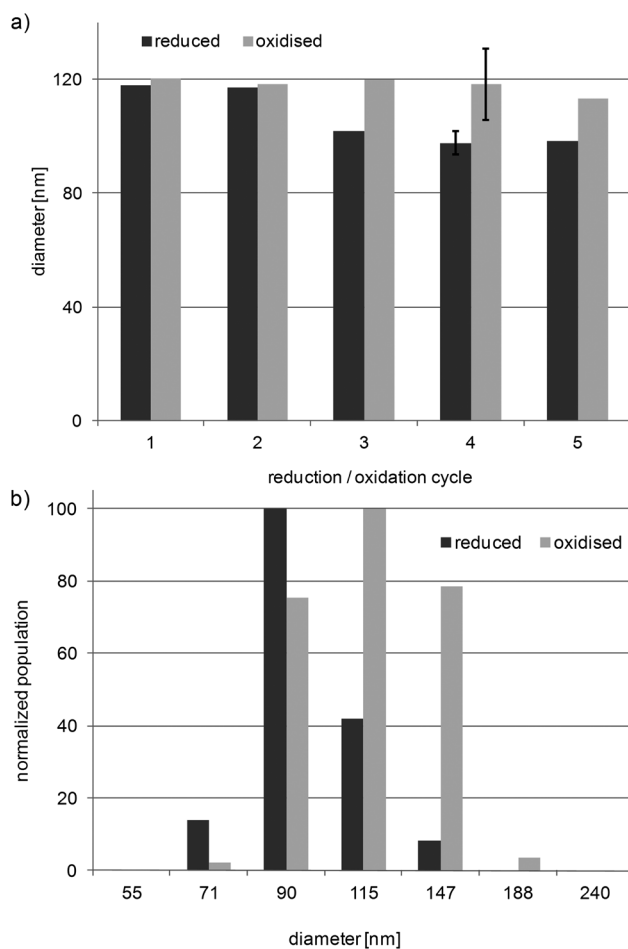


**Fig. 3** (a) Average diameter of PFS micelles composed of polymer **3** as measured by DLS. Data were collected through five consecutive, chemically induced, reduction/oxidation cycles. Error bars represent the standard deviation from multiple measurements collected at the 4<sup>th</sup> redox cycle; and (b) size distribution of oxidized and reduced forms of micelles for the 4<sup>th</sup> cycle. Average size for the reduced form is 98 nm and is 118 nm for the oxidized form.

solubility of this molecule makes paclitaxel a good candidate for micellar delivery.<sup>25</sup> Encapsulation of this drug into composite micelles of polymer **3** was achieved by the same way as for Nile Red. Release was studied based on the HPLC analysis, following established protocols.<sup>26</sup> Two different concentrations of iron chloride(III) were investigated with no-oxidant reference sample (Fig. 6).

As displayed in Fig. 6, the release profile strongly depends on the concentration of the oxidizing agent at the initial stage of release. For longer release times release from the micelle remains at a stable constant rate, comparable to those for the control sample. Paclitaxel leaches rather slowly and only approximately 20% of the encapsulated drug is released for the higher  $\text{FeCl}_3$  concentration in 24 h. Paclitaxel is poorly soluble in water and even after oxidation of micelles and substantial reduction of the micelle hydrophobic character, most likely still remains partially encapsulated in the hydrophobic pockets.

To assess if PFS is adequate as a material for medical applications, toxicity tests on the Caco-2 human intestinal epithelial

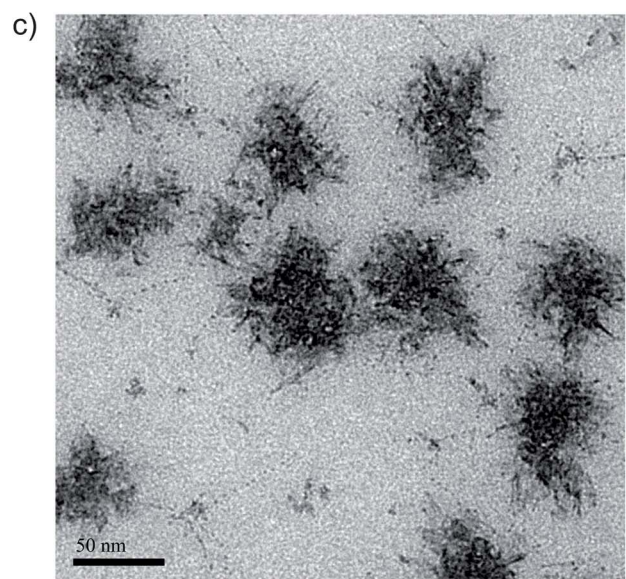
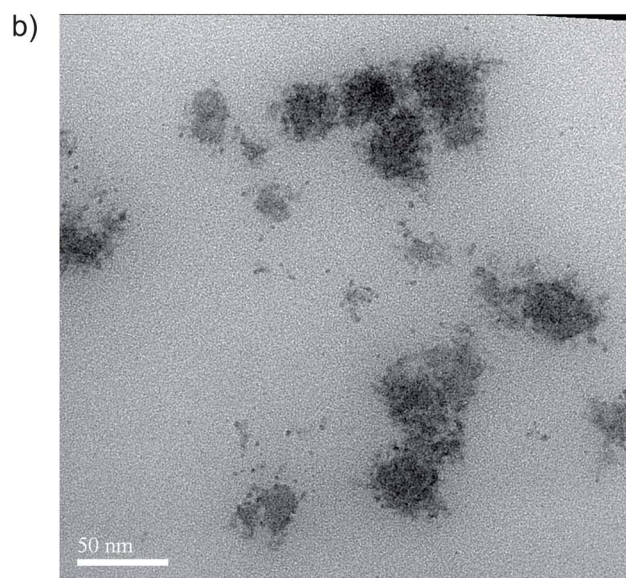
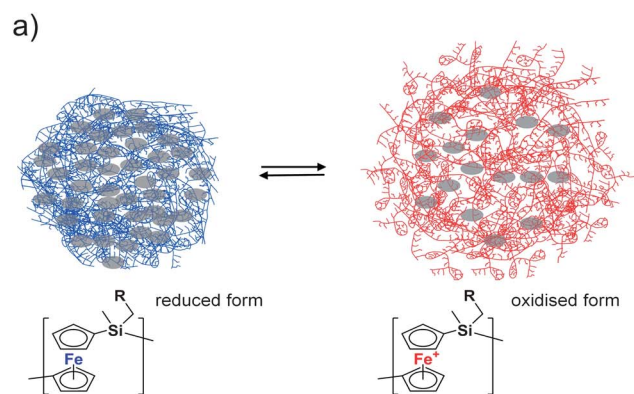


**Fig. 4** (a) Schematic cycle of micelle transformation upon oxidation and reduction with hydrophobic pockets represented as grey spots; (b) TEM micrograph of the reduced form of polymer 3; and (c) TEM micrograph of the oxidized form of polymer 3.

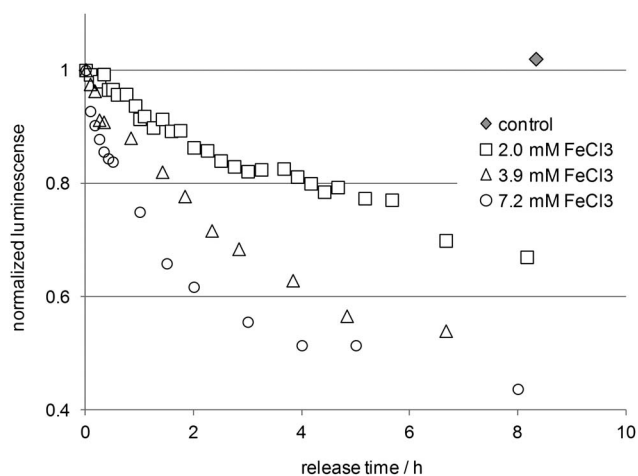


**Fig. 5** Normalized emission intensity of Nile Red (at 652 nm) encapsulated by polymer 3 in the presence of different amounts of FeCl<sub>3</sub>.

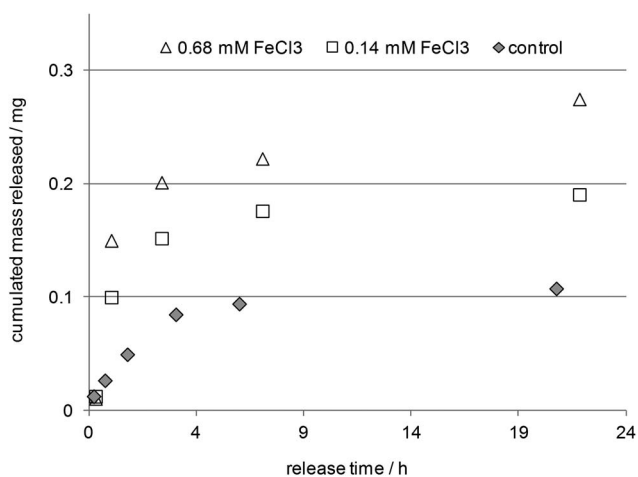


**Fig. 6** Release profiles of paclitaxel from polymeric micelle 3 for various concentrations of FeCl<sub>3</sub>.

cell line were performed.<sup>17</sup> The cellular conversion of MTT, a viability assay, showed that polymer 4 is not toxic to epithelial cells at 10  $\mu\text{g mL}^{-1}$  dose. In the presence of serum in treatment medium polymer 4 was non-toxic up to 30  $\mu\text{g mL}^{-1}$ . Above 30  $\mu\text{g mL}^{-1}$  concentration the viability of Caco-2 cells was reduced in a dose-dependent way (Table 1 and Fig. 7).

**Table 1** Toxic concentrations (TC) of polymers 3 and 4 determined by MTT and LDH release assays on Caco-2 cells. TC<sub>0</sub>: non-toxic concentration; TC<sub>100</sub>: concentration eliciting cell death similar to 1% Triton X-100 detergent used as positive control

		TC <sub>0</sub> /μg mL <sup>-1</sup>		TC <sub>100</sub> /μg mL <sup>-1</sup>	
		Serum free	Serum	Serum free	Serum
Polymer 4	MTT	10	30	60	100
	LDH	10	10	60	60
Polymer 3	MTT	3	10	60	60
	LDH	3	10	60	60

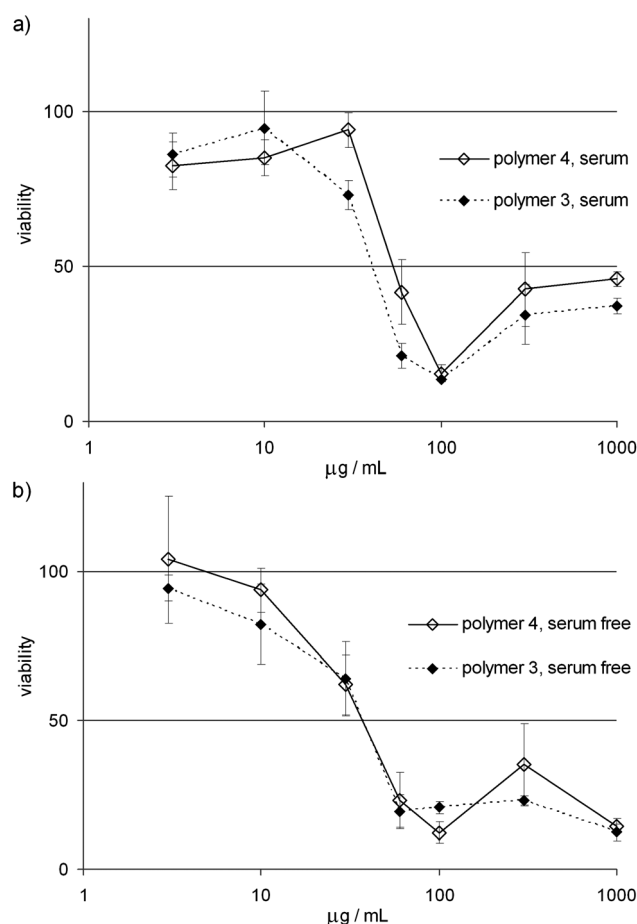


**Fig. 7** MTT viability assays of Caco-2 cells upon exposure to polymers 3 and 4 in (a) serum and (b) serum free culture medium.

**Table 2** Efficiency of DNA transfection compared to a commercially available polymer-based transfection reagent (Turbofect™ *in vitro* Transfection Reagent, Fermentas). Expression of the reporter was measured by flow cytometry in ChC3 cells after 24 h of incubation at 37 °C

TF. reagent	% of positive cells
Polymer 3 (1 mg mL <sup>-1</sup> )	2.6
Polymer 4 (1 mg mL <sup>-1</sup> )	0.3
Turbofect™	33.3
No reagent, DNA	0.3
No reagent, no DNA	0.3

No significant cytotoxicity was detected in the case of polymer 3 between 3 and 10 µg mL<sup>-1</sup> on epithelial cells. The polymer was clearly toxic at concentrations over 30 µg mL<sup>-1</sup>. The results of the MTT viability assay were supported by measurement of lactate dehydrogenase (LDH) release. Both polymers increased LDH release from Caco-2 cells into the extracellular space in a dose-dependent way. A maximal LDH release indicating 100% toxicity was observed for 4 and 3 at 60 µg mL<sup>-1</sup> dose and above. Both polymers display similar toxicity, which is lower than that of typical chemotherapeutic agents.<sup>27</sup>

DNA transfection experiments were carried out with both polymers 3 and 4 to assess their application. Despite identical

charge to molecule ratio, transfection efficiency is interestingly significantly higher for amphiphilic molecule 3 compared to polymer 4. Efficiency remains at rather moderate levels compared to a commercial transfection reagent (Table 2), however only the standard protocol of Turbofect™ was followed and reaction conditions for efficient DNA delivery in the case of polymers 3 and 4 were not optimized.

## Conclusions

A novel poly(ferrocenylsilane) amphiphilic oligomer was synthesised by ring opening polymerization of strained ferrocenophane and subsequent side chain modification. The polymer forms small 100 nm assemblies in water, displaying redox activated, reversible properties and morphology transformation upon change of the redox state. Low cell toxicity was observed below the concentration of 10 µg mL<sup>-1</sup>. The material was successfully tested as a delivery medium against paclitaxel and Nile Red showing a high degree of control over release kinetics upon variation of redox conditions. High increase in DNA transfection was observed comparing polymers with micellar 3 and not micellar 4 character. This result provides an interesting hint indicating suitability of this material for the design of novel DNA transfection vectors. Further application of PFS built vehicles needs understanding of polymeric chain fate, exposed to an intracellular chemistry, which will remain a subject of further evaluation.

## Acknowledgements

We are grateful to the A\*STAR (Agency for Science, Technology and Research), Singapore and NKTH—A\*STAR (Hungarian—Singaporean) Bilateral S&T International Cooperation (BIO-SPONA) TeT-08-SG-STAR for providing financial support.

## Notes and references

- M. Comellas-Aragones, H. Engelkamp, V. I. Claessen, N. A. J. M. Sommerdijk, A. E. Rowan, P. C. M. Christianen, J. C. Maan, B. J. M. Verduin, J. J. L. M. Cornelissen and R. J. M. Nolte, *Nat. Nanotechnol.*, 2007, **2**, 635–639; A. de la Escosura, R. J. M. Nolte and J. J. L. M. Cornelissen, *J. Mater. Chem.*, 2009, **19**, 2274–2278.
- H. Petry, C. Goldmann, O. Ast and W. Luke, *Curr. Opin. Mol. Ther.*, 2003, **5**, 524–528; B. A. Schroder, C. Wrocklage, A. Hasilik and P. Saftig, *Proteomics*, 2010, **10**, 4053–4076.
- M. Goldberg, R. Langer and X. Q. Jia, *J. Biomater. Sci., Polym. Ed.*, 2007, **18**, 241–268; S. Ganta, H. Devalapally, A. Shahiwala and M. Amiji, *J. Controlled Release*, 2008, **126**, 187–204; J. M. Berlin and J. M. Tour, *Nanomedicine*, 2010, **5**, 1487–1489; E. Amstad, J. Kohlbrecher, E. Muller, T. Schweizer, M. Textor and E. Reimhult, *Nano Lett.*, 2011, **11**, 1664–1670.
- H. F. Xu, F. H. Meng and Z. Y. Zhong, *J. Mater. Chem.*, 2009, **19**, 4183–4190; M. Benaglia, A. Alberti, E. Spisni, A. Papi, E. Treossi and V. Palermo, *J. Mater. Chem.*, 2011, **21**, 2555–2562.
- X. W. Zhu and M. H. Liu, *Langmuir*, 2011, **27**, 12844–12850; C. F. Di, X. S. Jiang, R. Wang and J. Yin, *J. Mater. Chem.*, 2011, **21**, 4416–4423.
- D. Janczewski, N. Tomczak, S. H. Liu, M. Y. Han and G. J. Vancso, *Chem. Commun.*, 2010, **46**, 3253–3255; D. Janczewski, N. Tomczak, M. Y. Han and G. J. Vancso, *Nat. Protoc.*, 2011, **6**, 1546–1553.
- V. P. Torchilin, *J. Controlled Release*, 2001, **73**, 137–172.
- R. Cheng, F. Feng, F. H. Meng, C. Deng, J. Feijen and Z. Y. Zhong, *J. Controlled Release*, 2011, **152**, 2–12.

- 9 C. A. Nijhuis, B. J. Ravoo, J. Huskens and D. N. Reinhoudt, *Coord. Chem. Rev.*, 2007, **251**, 1761–1780; G. R. Whittell, M. D. Hager, U. S. Schubert and I. Manners, *Nat. Mater.*, 2011, **10**, 176–188.
- 10 C. J. F. Rijcken, O. Soga, W. E. Hennink and C. F. van Nostrum, *J. Controlled Release*, 2007, **120**, 131–148; C. Ru, F. Feng, F. H. Meng, C. Deng, J. Feijen and Z. Y. Zhong, *J. Controlled Release*, 2011, **152**, 2–12.
- 11 A. N. Koo, H. J. Lee, S. E. Kim, J. H. Chang, C. Park, C. Kim, J. H. Park and S. C. Lee, *Chem. Commun.*, 2008, 6570–6572; L. Zhang, W. U. Liu, L. Lin, D. Chen and M. H. Stenzel, *Biomacromolecules*, 2008, **9**, 3321–3331; J. H. Ryu, R. Roy, J. Ventura and S. Thayumanavan, *Langmuir*, 2010, **26**, 7086–7092; V. Bulmus, M. Woodward, L. Lin, N. Murthy, P. Stayton and A. Hoffman, *J. Controlled Release*, 2003, **93**, 105–120.
- 12 Y. Takeoka, T. Aoki, K. Sanui, N. Ogata, M. Yokoyama, Y. Okano, Y. Sakurai and M. Watanabe, *J. Controlled Release*, 1995, **33**, 79–87; Z. P. Xiao, Z. H. Cai, H. Liang and J. Lu, *J. Mater. Chem.*, 2010, **20**, 8375–8381; D. Correia-Ledo, A. A. Arnold and J. Mauzeroll, *J. Am. Chem. Soc.*, 2010, **132**, 15120–15123; Q. Yan, J. Y. Yuan, Z. N. Cai, Y. Xin, Y. Kang and Y. W. Yin, *J. Am. Chem. Soc.*, 2010, **132**, 9268–9270.
- 13 V. Bellas and M. Rehahn, *Angew. Chem., Int. Ed.*, 2007, **46**, 5082–5104; D. E. Herbert, U. F. J. Mayer and I. Manners, *Angew. Chem., Int. Ed.*, 2007, **46**, 5060–5081.
- 14 Z. Y. Zhong, C. Lin, Y. Ma, M. A. Hempenius, M. C. Lok, M. M. Fretz, J. F. J. Engbersen, G. J. Vancso, W. E. Hennink and J. Feijen, *J. Controlled Release*, 2006, **116**, e81–e83; I. J. Minten, Y. J. Ma, M. A. Hempenius, G. J. Vancso, R. J. M. Nolte and J. J. L. M. Cornelissen, *Org. Biomol. Chem.*, 2009, **7**, 4685–4688.
- 15 Y. J. Ma, W. F. Dong, M. A. Hempenius, H. Mohwald and G. J. Vancso, *Nat. Mater.*, 2006, **5**, 724–729; Y. J. Ma, W. F. Dong, M. A. Hempenius, H. Mohwald and G. J. Vancso, *Angew. Chem., Int. Ed.*, 2007, **46**, 1702–1705.
- 16 K. N. Power-Billard, R. J. Spontak and I. Manners, *Angew. Chem., Int. Ed.*, 2004, **43**, 1260–1264; T. Gadt, N. S. Jeong, G. Cambridge, M. A. Winnik and I. Manners, *Nat. Mater.*, 2009, **8**, 144–150; J. F. Gohy, B. G. G. Lohmeijer, A. Alexeev, X. S. Wang, I. Manners, M. A. Winnik and U. S. Schubert, *Chem.–Eur. J.*, 2004, **10**, 4315–4323; S. F. M. Yusoff, J. B. Gilroy, G. Cambridge, M. A. Winnik and I. Manners, *J. Am. Chem. Soc.*, 2011, **133**, 11220–11230.
- 17 A. Szuts, P. Láng, R. Ambrus, L. Kiss, M. A. Deli and P. Szabó-Révész, *Int. J. Pharm.*, 2011, **410**, 107–110.
- 18 R. J. Puddephatt, *J. Inorg. Organomet. Polym. Mater.*, 2005, **15**, 371–388.
- 19 D. A. Foucher, B. Z. Tang and I. Manners, *J. Am. Chem. Soc.*, 1992, **114**, 6246–6248.
- 20 M. A. Hempenius and G. J. Vancso, *Macromolecules*, 2002, **35**, 2445–2447.
- 21 M. A. Hempenius, N. S. Robins, R. G. H. Lammertink and G. J. Vancso, *Macromol. Rapid Commun.*, 2001, **22**, 30–33; M. A. Hempenius, F. F. Brito and G. J. Vancso, *Macromolecules*, 2003, **36**, 6683–6688.
- 22 Y. J. Ma, W. F. Dong, E. S. Kooij, M. A. Hempenius, H. Mohwald and G. J. Vancso, *Soft Matter*, 2007, **3**, 889–895; J. Song and G. J. Vancso, *Langmuir*, 2011, **27**, 6822–6829.
- 23 M. C. A. Stuart, J. C. van de Pas and J. B. F. N. Engberts, *J. Phys. Org. Chem.*, 2005, **18**, 929–934; J. F. Deye, T. A. Berger and A. G. Anderson, *Anal. Chem.*, 1990, **62**, 615–622.
- 24 E. K. Rowinsky and R. C. Donehower, *N. Engl. J. Med.*, 1995, **332**, 1004–1014.
- 25 G. S. Kwon, *Crit. Rev. Ther. Drug Carrier Syst.*, 2003, **20**, 357–403.
- 26 C. L. Lay, H. Q. Liu, D. C. Wu and Y. Liu, *Chem.–Eur. J.*, 2010, **16**, 3001–3004; C. L. Lay, H. Q. Liu, H. R. Tan and Y. Liu, *Nanotechnology*, 2010, **21**, 065101.
- 27 J. Lieber, C. Eicher, J. Wenz, B. Kirchner, S. W. Warmann, J. Fuchs and S. Armeanu-Ebinger, *BMC Cancer*, 2011, **11**, 362.